

Scanning tunneling microscopy and photoemission from Fe/Cu(111)

A. Brodde, K. Dreps, J. Binder, Ch. Lunau, and H. Neddermeyer

Institut für Experimentalphysik der Ruhr-Universität Bochum, D-4630 Bochum, Federal Republic of Germany

(Received 20 August 1992)

Using scanning tunneling microscopy and angle-resolved uv photoemission, we have measured thin films of Fe on Cu(111) in the coverage range between 0.03 and 5 monolayers. Our results show that under the experimental conditions used (substrate temperature between room temperature and 300°C) the Fe deposit condenses in the form of three-dimensional islands. Only at the nucleation stage are two-dimensional Fe structures with monatomic height observed on the surface. Fe preferentially condenses at step edges on the upper terrace. We see indications of Fe-induced diffusion of Cu atoms already at room temperature. The shape of the Fe islands provides evidence for the growth of Fe islands in the form of fcc Fe(111) layers. The photoemission results exhibit distinct differences in the electronic states below the Fermi level for the 1-monolayer and 5-monolayer film, which, in our opinion, are representative of a thin fcc Fe(111) film and bulk fcc Fe(111), respectively.

I. INTRODUCTION

The nearest-neighbor distances of Cu and Fe atoms in their bulk fcc and bcc structures, respectively, are sufficiently similar ($d_{\text{Cu}}=2.56 \text{ \AA}$, $d_{\text{Fe}}=2.48 \text{ \AA}$) (Ref. 1) to expect pseudomorphic growth of fcc (γ) Fe layers in (111) orientation on Cu(111). Thin films of γ -Fe(111) are of considerable interest in the field of surface magnetism.²⁻⁴ The magnetic properties could be completely different from the case of bcc (α) Fe. In the first study of magnetism of Fe layers on Cu(111) Kümmerle and Gradmann found at room temperature (RT) ferromagnetism and a surprisingly small magnetic moment of $0.58\mu_B/\text{atom}$.² In contrast, Mössbauer studies of thin Fe films indicated paramagnetism at RT and a transition to antiferromagnetism at low temperatures.³ In a later work using electron capture spectroscopy Rau *et al.* again found long-range ferromagnetic order at RT for a film of 4 monolayers (ML) and a short-range ferromagnetic order of a 1-ML film.⁴

It has been pointed out in Ref. 2 that the magnetism of thin Fe films may drastically depend on their structural properties. Since the morphology of a film is determined in part by deposition conditions such as substrate temperature, atom flux from the evaporation source, structural characteristics of the substrate, and possible presence of contamination, the structure of the Fe deposit may actually be quite different in the various experiments and give rise to the observed discrepancies in the magnetic order. In the first low-energy electron-diffraction (LEED) and Auger-electron spectroscopy (AES) study of Fe/Cu(111), layer-by-layer growth of Fe films in the fcc structure was found at RT up to a thickness of about 8 Å; for thicker films the formation of α -Fe crystallites was observed.⁵ These results were later confirmed using LEED/AES by Darici *et al.*⁶ and recently by Tian, Jona, and Marcus.⁷ It is clear, however, that LEED/AES results cannot provide as accurate information on details of the growth mode as, for example, on the island structure, which, on

the other hand, would determine the magnetic properties of the films to a large extent. We have therefore performed a combined study using scanning tunneling microscopy (STM) and angle-resolved ultraviolet photoelectron spectroscopy (ARUPS) on the Fe/Cu(111) system in the monolayer (ML) coverage range. The comparison between STM and ARUPS results is interesting for a number of reasons. The most important is the intimate relation between structure and the electronic states of a material. Although the influence of the magnetic order on the electronic structure as revealed by ARUPS is normally quite weak, differences in the ARUPS results obtained from the Fe films in comparison with those of bcc single-crystal surfaces of Fe (Ref. 8) turned out to be quite drastic and may be analyzed in terms of the expected magnetic behavior.

A main aim of the present work is a characterization of Fe on Cu(111) with regard to the general growth mode up to a coverage (Θ) of approximately 5 ML ($\Theta=5$). We discuss the influence of the substrate temperature and of the Fe flux with regard to the macroscopic nature of the deposit. In contrast to the above-cited LEED/AES results, our STM work clearly shows that Fe does not grow in a layer-by-layer mode but rather forms three-dimensional (3D) islands, whose shape is particularly sensitive to the substrate temperature.⁹ Coalescence of the Fe islands was not yet achieved in this range of coverage.

II. EXPERIMENT

The experiments have been performed by using two different instrumental equipments for STM and ARUPS. Details of the STM (Ref. 10) and the photoemission apparatus¹¹ have already been described previously. Therefore, only some basic features of the experimental facilities and the differences in STM and ARUPS work will be summarized here.

The STM is equipped with a LEED optics, an electron energy analyzer for AES measurements, and facilities for

in situ sample preparation (ion bombardment, heating and effusion cell for Fe deposition). For the STM measurements constant current topographies (CCT's) have been recorded for a sample bias voltage U and a tunneling current I as given in the figure captions. The CCT's are displayed as usually in the form of gray tone images, where bright parts correspond to protrusions and dark parts to depressions.

The photoelectron spectrometer has an energy resolution ΔE of better than 60 meV full width at half maximum (FWHM) and an angle resolution of 2° (half angle of acceptance cone). The spectrometer is used without retarding the photoelectrons, which means that the energy resolution is a linear function of the kinetic energy E of the electrons ($\Delta E/E = \text{const}$). Radiation is obtained from a rare-gas resonance lamp and the results reported here are obtained by using He I resonance radiation (21.22 eV). The angle-resolved energy distribution curves of the photoelectrons (AREDC's) are measured either normal to the surfaces or by rotating the sample, the angle between incident radiation and electron emission being always constant. They are plotted against the initial energy referring to the Fermi level $E_F = 0$.

The Cu(111) substrates were oriented using standard Laue technique within an accuracy of 0.5° . After mechanical and chemical polishing they were mounted on a Ta (Mo) sample holder for the STM (ARUPS) measurements. *In situ* preparation consisted in cycles of Ar⁺ bombardment and annealing to 600°C until with AES contamination could no longer be detected. A clear LEED pattern with the threefold symmetry of Cu(111) was finally observed.

Fe (nominal cleanliness 99.999%) was deposited onto the Cu substrates in both experiments by using water-cooled Knudsen-type effusion cells with alumina crucible. To change the deposition rate in the STM experiments we have operated the Fe source at various temperatures (between 895 and 970°C), which produced deposition rates between 0.3 and 6 ML/min [referred to the number of substrate atoms in Cu(111)]. The deposition rates were measured by means of a quartz film thickness monitor, however in some of the STM experiments the quartz crystal was not oriented properly with respect to the Fe atomic beam, which means that the ML scale in the STM experiments has an estimated accuracy of only 20%. The base pressure of the STM system is in the low 10^{-11} -mbar range. During Fe evaporation in the STM chamber the pressure increased up to a value between 2×10^{-10} and 6×10^{-10} mbar. For each deposition experiment the substrate was recleaned by the above-mentioned cleaning procedure. The substrate was normally kept at RT; in some STM experiments the influence of an elevated substrate temperature (approximately 150 and 300°C) was investigated. Heating was accomplished by radiation from a filament and the temperature determined in a separate experiment by means of a thermocouple, which was temporarily attached to the sample holder. The accuracy of the given temperature therefore only allows establishment of the general effects in the growth mode of the Fe deposit. It was not intended in the present experiment to analyze more quantitatively the temperature

dependence of the island shape in order to learn more on the energetics of nucleation and island growth.

For photoemission the vacuum conditions were somewhat worse than for STM; the base pressure of the ARUPS measuring chamber is about 1×10^{-10} mbar. For ARUPS the Fe films were produced in the preparation chamber at a rate of approximately 0.3 ML/min. Although the pressure increase during evaporation was quite large (up to 1×10^{-8} mbar) in this case, the AES spectra did not show the presence of additional species on the surface. However, for the thicker films ($\Theta = 4$ and 5) a small contamination could not be ruled out completely as was concluded from the presence of a contamination-induced feature at -6 eV in the AREDC's. For the thinner films ($\Theta \leq 2$) the presence of characteristic surface-state emission from the Cu substrate confirmed sufficient cleanliness of the surfaces.

III. RESULTS

A. STM

Overview images of clean Cu(111) showed the presence of mostly monatomic steps [Fig. 1(a)]. The terrace structure became rougher (on the scale of 1000 Å) during the course of the experiments, probably due to the sputtering process and the formation of pinning centers for steps [see, for example, at P in Fig. 1(a)]. These pinning centers are frequently seen by STM on single-crystal surfaces and their chemical nature can hardly be identified, since they cover only a minor fraction of the surface. Nevertheless, they play an important role for the macroscopic shape of the surface, since they increase the length of the steps. In Fig. 1(a) two screw dislocations are also visible (e.g., at S).

On the clean substrate surface an atomic corrugation due to the dense-packed Cu atoms could be observed without difficulties [Fig. 1(b)]. This allowed us to accurately determine the high-symmetry directions on the sample and to estimate the concentration of chemisorbed species on the surface, which was actually very low, as could be concluded indirectly from the fact that the surface showed a regular pattern without local defects over typically 100×100 atomically resolved protrusions.

At the lowest coverage of our experiments ($\Theta = 0.03$) for RT deposition Fe condenses in small mostly oblong islands with a typical lateral size of $10 \times 30 \text{ \AA}^2$ and a height above the Cu(111) substrate of 2.0–2.2 Å (Fig. 2). The measured height indicates two-dimensional (2D) growth at this coverage. Assuming a close-packed arrangement of Fe atoms in the islands [consistent with the theoretical height of monatomic steps on γ -Fe(111) of 2 Å] the number of Fe atoms in the smallest islands (e.g., at A in the figure) may be estimated to be in the order of 60 atoms. Since smaller islands are not identified and a number of islands are already distinctly larger, the smallest islands could be the critical nuclei. On the large terrace in the center of the CCT the mean nearest-neighbor distance between the islands is $\approx 150 \text{ \AA}$, which corresponds approximately to the diffusion length of the Fe atoms on the Cu(111) substrate. On the step edges the

mean separation between the Fe islands is distinctly smaller ($\approx 80 \text{ \AA}$), i.e., Fe preferentially condenses on step edges. A surprising observation is that these islands are located on top of the step and not at the bottom on the lower terrace. The latter adsorption site would be expected intuitively as the preferred one and is actually observed for other systems [e.g., for Ag on Ni(100) (Ref. 12)].

Increasing the coverage to $\Theta=0.05$ gives rise to characteristic changes of the growth mode (Fig. 3). The Fe atoms almost exclusively condense on step edges and the height of the Fe islands with a typical lateral extension of $40 \times 40 \text{ \AA}^2$ is mostly at least 4 \AA , which definitely

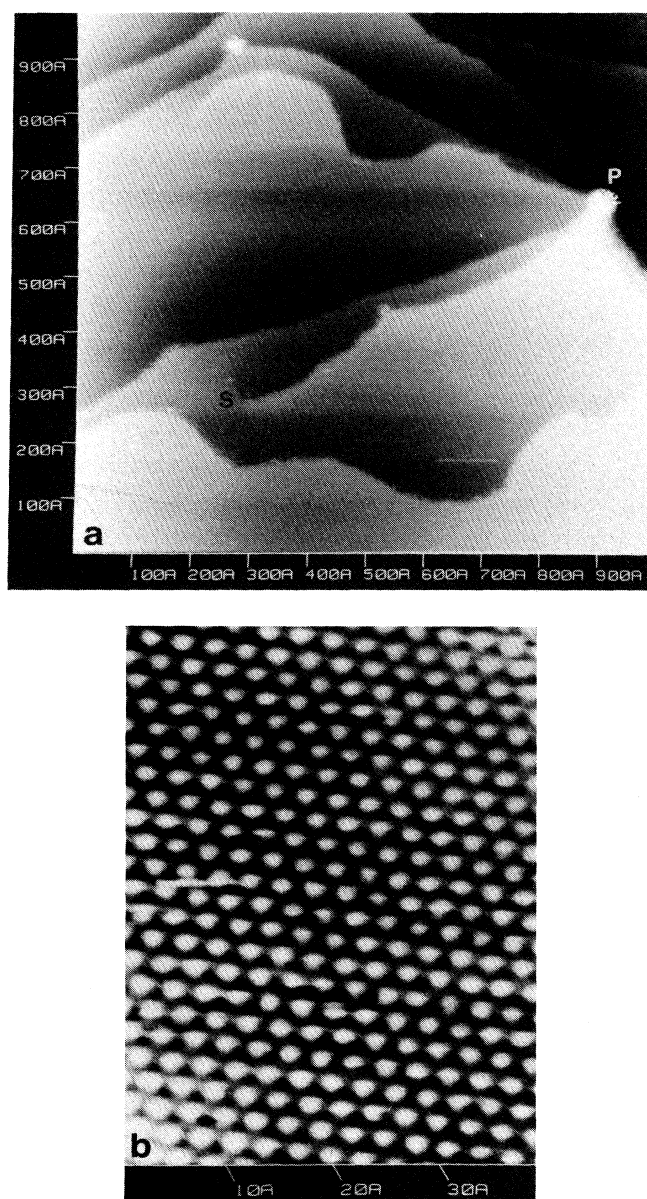


FIG. 1. CCT from clean Cu(111) acquired with $U = -0.1 \text{ V}$ and $I = 0.5 \text{ nA}$ (a) and $U = -1.25 \text{ V}$ and $I = 0.5 \text{ nA}$ (b).

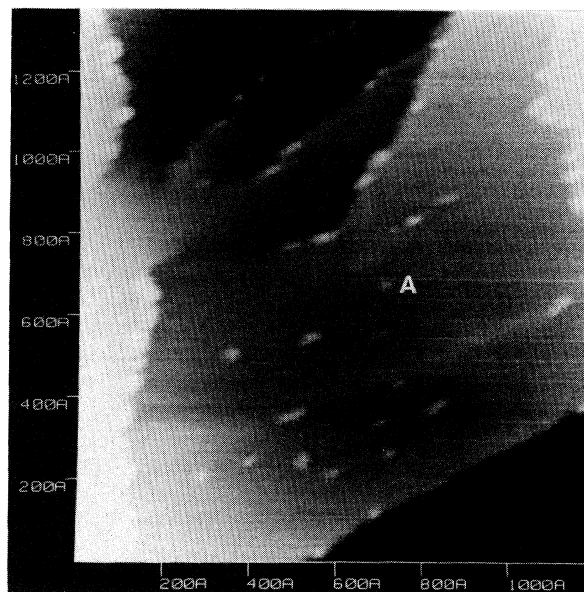


FIG. 2. CCT from 0.03-ML Fe on Cu(111) deposited at RT acquired with $U = -0.05 \text{ V}$ and $I = 0.5 \text{ nA}$.

corresponds to a thickness of at least 2 ML and therefore indicates the onset of the 3D growth mode. One observation of this image is striking: hexagonal holes of monatomic height (2 \AA) due to an area of removed Cu atoms are seen which look very similar to those obtained by Michely *et al.* on Pt(111) in a systematic study of the

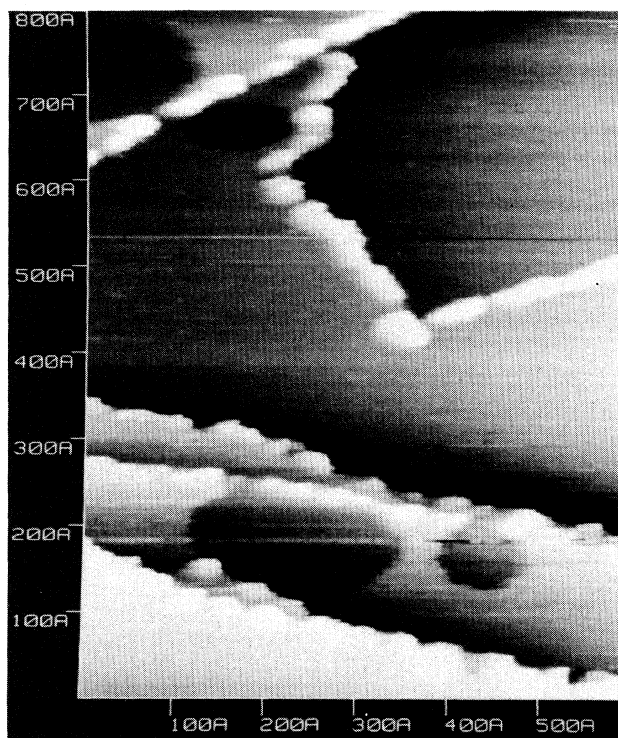


FIG. 3. CCT from 0.05-ML Fe on Cu(111) deposited at RT acquired with $U = 0.05 \text{ V}$ and $I = 0.5 \text{ nA}$.

sputtering effect by Ar ions.¹³ The observation of holes in the Cu substrate in our experiments could in principle also be explained by the influence of Ar-ion sputtering during sample preparation. In this case the holes would already be present during Fe deposition and should be decorated with Fe islands, which is obviously not seen on the image. Moreover, the uncovered substrate surface prepared in the same way never showed such holes. We therefore have to conclude that the holes in the Cu(111) substrate are formed during the deposition process. Since similar structures are even more pronounced if a substrate temperature of 150 °C is used (see below) and for deposition experiments of Fe on Cu(100) using higher substrate temperatures,¹⁴ we infer that the adsorption of Fe atoms may give rise to diffusion of Cu atoms.

For $\Theta=0.5$ (Fig. 4) the growth continues by increasing the lateral size (typically 125 Å) of the Fe islands and their height mainly to values between 4 and 6 Å equivalent to 2–3 ML. The characteristic holes of removed Cu atoms in the substrates are again visible. It is interesting to note that they are preferentially located very close to steps, which are indirectly visualized by the decoration with Fe islands. This would indicate that the removed Cu atoms are incorporated into steps of the substrate. The Fe islands on the terraces have a nearest-neighbor distance of ≈ 210 Å, which is only slightly larger than for $\Theta=0.03$. The general shape of the Fe islands is not very regular although a preferential growth direction, which may be different for the individual islands, is present in many cases.

In Fig. 5 an overview image for $\Theta=2$ and RT condensation is reproduced. Roughly 50% of the substrate surface is now covered with Fe islands. The lateral size of the Fe islands has slightly increased against $\Theta=0.5$, in particular of those islands, which decorate the step edges,

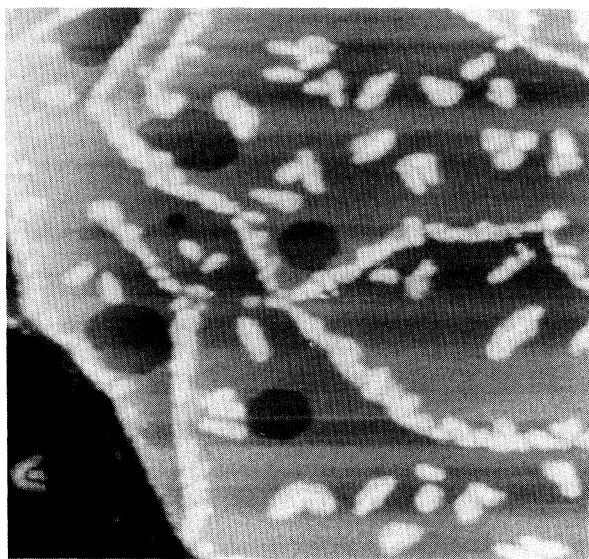


FIG. 4. CCT from 0.5-ML Fe on Cu(111) deposited at RT acquired with $U=0.05$ V and $I=0.5$ nA. The surface area is 2000×2000 Å².

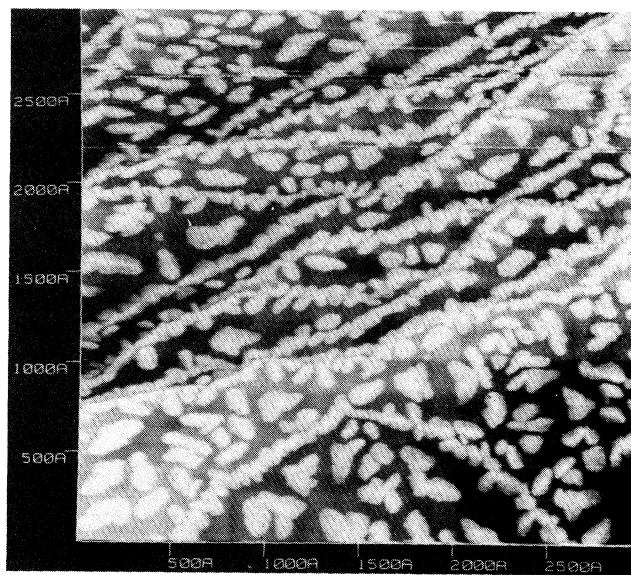


FIG. 5. CCT from 2-ML Fe on Cu(111) deposited at RT acquired with $U=0.05$ V and $I=0.5$ nA.

where the growth proceeds mostly in a direction away from the steps. The nearest-neighbor distance of Fe islands on larger terraces was found to be typically 110 Å. The corrugation over Fe islands is in the range of 4–10 Å showing again the 3D nature of the growth mode. The macroscopic distribution of Fe islands is essentially determined by the step and terrace structure of the surface. Absence of layer-by-layer growth mode for room-temperature deposition is evident.

In the course of the experiments we have investigated the influence of the substrate temperature on the growth mode during Fe deposition. Our main result is that for 150 and 300 °C the general growth mode remains unaffected. Only the shape of the 3D islands experiences distinct changes. In Fig. 6 an overview image for $\Theta=4$ and a substrate temperature of 300 °C is displayed. The main difference to the results obtained for RT deposition is that the shape of the individual Fe islands is more compact. If we consider the islands on the terraces we realize that for the higher substrate temperature the Fe islands very often show hexagonal or triangular shape. The island density on the terraces is ≈ 135 Å², which appears to be somewhat larger than for RT deposition and higher coverage.

In Fig. 7 a high-resolution CCT for $\Theta=3$ and a substrate temperature of 150 °C is displayed, where the regular shape of the islands can be recognized. We see that the islands reflect the threefold symmetry of the substrate. The direction of the edges coincides with the high-symmetry directions of the substrate [as could be concluded from a measurement showing the atomic structure of the substrate; see Fig. 1(b)]. The agreement can only be explained by the formation of fcc Fe(111), because the directions of two of the edges of bcc Fe(110) is-

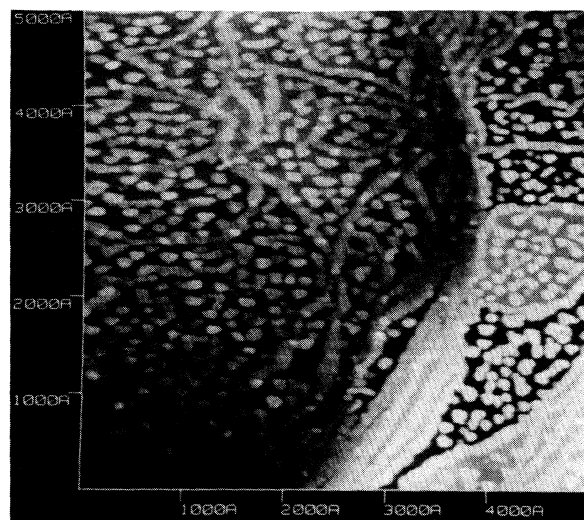


FIG. 6. CCT from 4-ML Fe on Cu(111) deposited at 300°C acquired with $U = -0.1$ V and $I = 0.5$ nA.

lands would not coincide with symmetry directions, if one edge is oriented along $[\bar{1}01]$.⁹ For the height of the islands we find values between 5 and 15 Å corresponding to at least 2–7 Fe(111) layers in the fcc structure. We note that some of the steps found on top of the islands are very close to 2 Å (see, e.g., at x) again consistent with the growth of fcc Fe(111) crystallites.

In Fig. 8 a CCT from Fe on Cu(111) is reproduced, which, in our opinion, is characteristic for a stepped area of the substrate and shows the effects of Cu diffusion during condensation of the Fe deposit at higher substrate

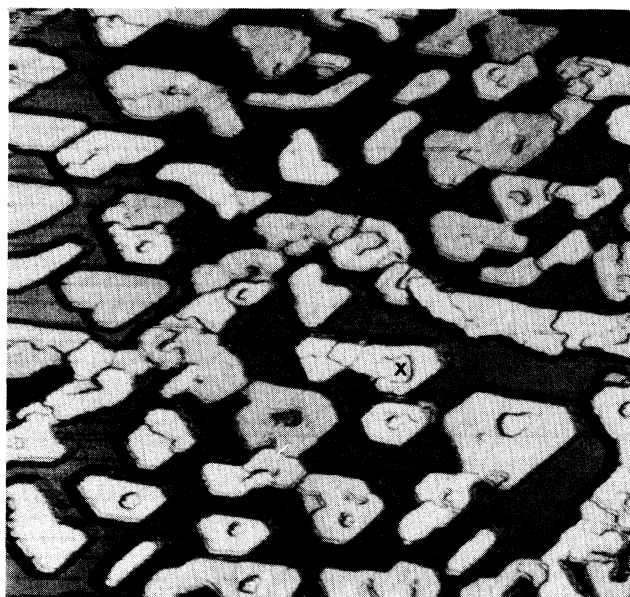


FIG. 7. CCT from 3-ML Fe on Cu(111) deposited at 150°C acquired with $U = -0.05$ V and $I = 0.5$ nA. The surface area is $1500 \times 1500 \text{ \AA}^2$. The uncovered Cu(111) substrate is represented in the intermediate gray tone level.

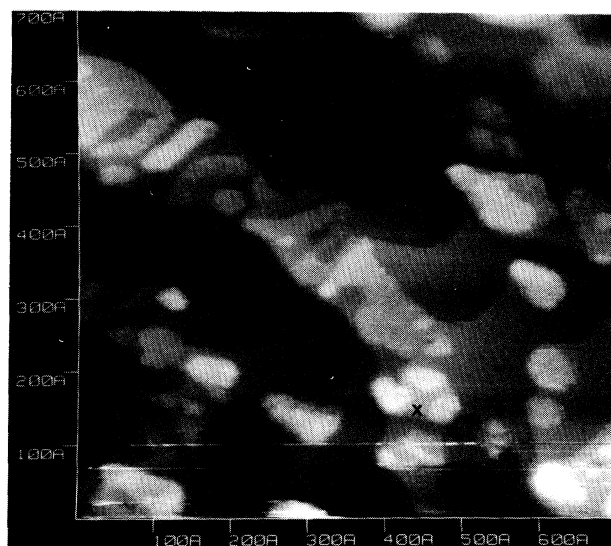


FIG. 8. CCT from ≈ 1 -ML Fe (the local coverage is smaller, in our opinion) on Cu(111) deposited at 150°C acquired with $U = -0.05$ V and $I = 50$ nA.

temperatures (150°C). The nominal Fe coverage is in the order of $\Theta = 1$ but locally seems to be much smaller. On the basis of the shape of the islands on top of the terraces we conclude that the islands cannot only be composed of Fe atoms. Since for this part of the sample a large number of Cu holes have been formed, the excess Cu atoms must be found somewhere and we believe that in addition to edge sites they may also form a new layer on top of a terrace. For example, the island with threefold symmetry labeled x actually consists of a basis and three smaller islands each of monatomic height. We assign the basis to Cu and the three small islands to Fe atoms. In other words, the deposition of Fe atoms induces a kind of roughening of the substrate surface, whose atomic nature is not yet fully understood. Since the effects are predominantly observed on stepped parts of the surface, we suggest that they are related to an exchange of Cu and Fe atoms or to an excitation of a terrace Cu atom during the initial Fe adsorption steps, where the adsorption energy has to be annihilated. After completion of the Fe deposition only near a substrate step the Fe-induced fluctuation of Cu atoms may become observable as macroscopic change of the substrate structure. We note that in the case of Fe/Cu(100) these kinds of effects are even more pronounced and the roughening of Cu step edges by removal of Cu atoms is obvious.¹⁴

Finally, we mention our experiments using different Fe fluxes for deposition on a RT substrate. Actually, we did not find clear differences in the morphology of the films up to a coverage of a few ML for deposition rates between 0.3 and 6 ML/min.

B. ARUPS

In the present work we show three sets of measurements. In the first set (Fig. 9) the general development of

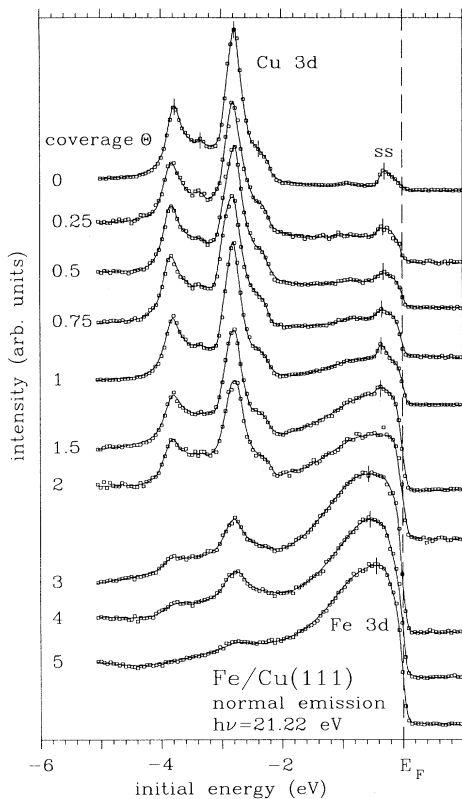


FIG. 9. AREDC's from Fe/Cu(111) as a function of Fe coverage.

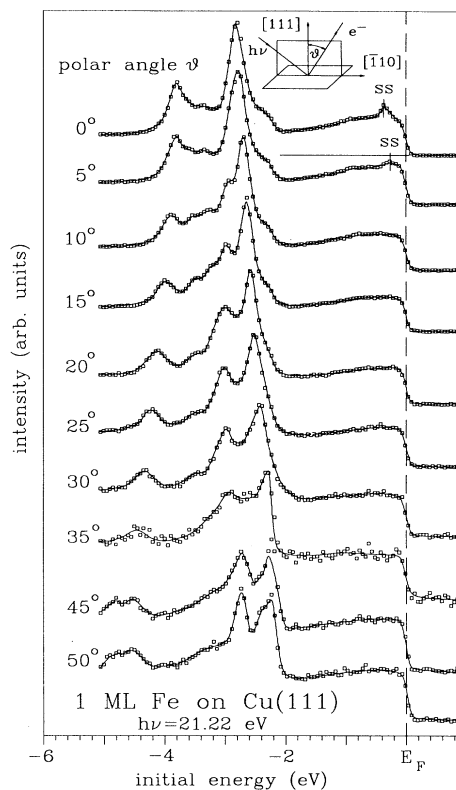


FIG. 10. AREDC's from 1-ML Fe and Cu(111) obtained as a function of polar angle of emission.

the surface electronic structure as revealed by normal emission with increasing film thickness ($\Theta=0-5$) and some information on the growth mode is contained. Two additional sets demonstrate the dependence of the AREDC's on the polar angle ϑ of emission for $\Theta=1$ (Fig. 10) and $\Theta=5$ (Fig. 11) in order to establish whether any 2D or 3D dependency of the electronic structure of the Fe deposit is present.

Since the films have been prepared in a different system under similar preparation conditions as for the STM measurements, the structural properties as extracted from LEED, AES, and ARUPS should be described briefly. Absence of layer-by-layer growth mode for room-temperature deposition can be deduced from the intensity decrease of Cu 3d emission with increasing Fe film thickness (Fig. 9) although the intensity reduction from $\Theta=4$ to $\Theta=5$ seems to be higher than would be expected from the behavior at lower coverages. The AES intensity ratio of Cu $M_{2,3}VV$ and Fe $M_{2,3}VV$ transitions was consistent with a 3D island growth mode. In LEED the 1×1 pattern of Cu(111) was visible up to $\Theta=3$. For higher coverages distinct LEED spots were no longer visible in an increased background of scattered electrons. The long-range order of the films cannot be very high, therefore. Qualitatively, the LEED results are consistent with the STM measurements as reproduced in Fig. 5, where the Fe islands are probably too small and their heights not of sufficient homogeneity to produce coherent

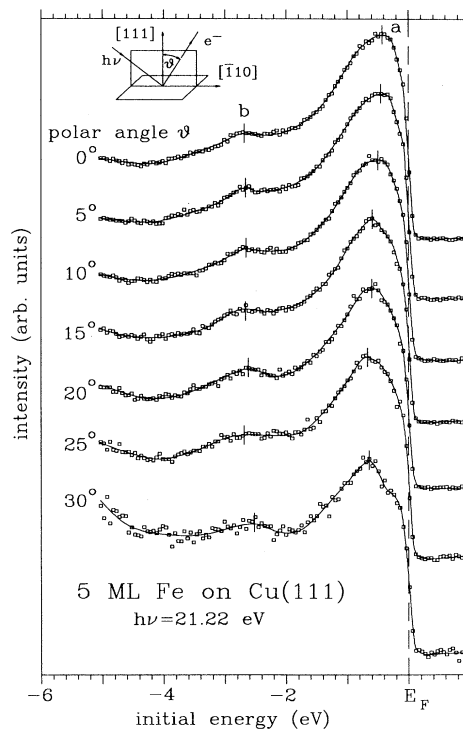


FIG. 11. AREDC's from 5-ML Fe on Cu(111) obtained as a function of polar angle of emission.

contributions to a diffraction pattern. Nevertheless, in comparison with our STM images we expect local order, registry with the substrate surface, and growth of fcc Fe(111) crystallites on a lateral scale of 100 Å. Our photoemission results from the 5-ML Fe film (see below) support such a growth mode.

The normal-emission AREDC's of Fe/Cu(111) show for the clean substrate the well-known surface state in the *sp* band gap¹⁵ labeled *ss* in Fig. 9 and below -2 eV transitions from the bulk Cu *d* bands. The deposited Fe atoms give rise to emission, which is essentially concentrated directly below E_F . Emission from the Cu surface state *ss* is visible up to $\Theta=1.5$ (for $h\nu=16.85$ eV also clearly for $\Theta=2$), which shows that the condensed Fe atoms do not cover the surface completely. For $\Theta=3-5$ the Fe states exhibit a maximum 0.4–0.6 eV below E_F and no distinct fine-structure details.

Since the surface state *ss* from Cu(111) disperses upwards with increasing polar angle ϑ of emission and passes E_F at $k_{\parallel}=0.25 \text{ \AA}^{-1}$,¹⁶ the contribution of the Fe 3*d* states undistorted by overlapping transitions from Cu can be determined from AREDC's obtained at larger polar angle of emission (Figs. 10 and 11). Moreover, ordering in the Fe films may be inferred from dispersion effects in the initial energy-band structure $E(\mathbf{k}_{\parallel})$ vs ϑ .

For $\Theta=1$ (Fig. 10) the surface state *ss* has indeed disappeared for $\vartheta=10^\circ$. The Fe-derived states are found as a broad structure whose maximum is located immediately below E_F and which do not show any distinct influence of the emission angle. For $\Theta=5$ (Fig. 11) the occurrence of a maximum (denoted *a*) definitely below E_F at -0.4 to -0.6 eV is seen for each AREDC. A small dependency on the polar angle ϑ is identified; it appears as a downward shift of the maximum (denoted *a*) with increasing ϑ . An additional weaker structure (labeled *b*) is found at about -2.6 eV rather independent on ϑ .

Although the effects in the Fe-derived states do not look very drastic, some effects are clear enough and have to be considered for the discussion. (i) For small coverages ($\Theta \approx 1$) dispersion effects for $E(\mathbf{k}_{\parallel})$ are absent, while at the same time the AREDC's provide evidence for a density-of-states maximum of the Fe states at or even above E_F . (ii) For higher coverages ($\Theta=5$) a distinct maximum in the AREDC's below E_F indicates the presence of a density-of-states maximum at -0.4 to -0.6 eV. Small dispersion effects indicate sufficient order in the oriented Fe crystallites. It should be noted that AREDC's obtained for $h\nu=16.85$ eV on the same systems (not shown here) provide the same information.

IV. DISCUSSION

The experimental work in the literature on Fe/Cu(111) in the monolayer coverage range and the substrate being at room temperature or at most a few hundred K above during Fe deposition is commonly interpreted in terms of an initial layerlike growth mode of the deposit. Our STM and ARUPS results did not confirm such behavior but rather showed a 3D growth mode already for small coverages ($\Theta=0.05$). Only during the nucleation stage of the deposit could 2D Fe clusters be identified on the sub-

strate surface. The Fe islands preferentially condense at step edges but on the upper terrace, which is believed to be quite unusual, since the number of nearest neighbors on the lower terrace would be larger and the adsorption energy should be higher there. The fact that a minimum of the potential for Fe adsorption is lowest on top of a step could be related to a particular large charge transfer from the high-lying to the low-lying Cu atoms, which leads to a general smoothing of the electronic charge density at a step. The degree of smoothing effect would then determine whether condensation occurs on the upper or lower terrace. It has already been mentioned that for another heterosystem [Ag/Ni(100)] initial condensation is found at step edges on the lower terrace.¹²

The direction of the edges of the Fe islands indicates growth in the fcc lattice. Monatomic steps on the Fe islands at a height of 2 Å and their flatness are also consistent with the growth of fcc (γ) Fe(111) in the range of $\Theta \leq 5$, which was the largest coverage studied in the present experiments. This fact is in agreement with published LEED work.⁵⁻⁷ We note that we have attempted to obtain atomically resolved STM images on the Fe islands in order to confirm directly the fcc (111) structure of the Fe deposit. The results (not shown here) were less satisfactory than those from clean Cu(111) [see Fig. 1(b)] due to tip instabilities, which are frequently found on stepped surfaces, and lack of resolution in this case. We did observe in some of the measurements the presence of rows of atomic features, whose orientation agreed with those of the [110]-like symmetry directions of Cu(111). However, since the lateral extension of these ordered structures was only 20–30 Å their presence may not be convincing evidence for the growth of fcc Fe(111) but is certainly consistent with such a growth mode.

In Ref. 6 it has been emphasized that Cu segregation may occur on Fe/Cu(111) at relatively low temperatures (200°C). Our STM results provide evidence that indeed an Fe-induced diffusion of Cu atoms may produce holes in the substrate, while the excess Cu atoms probably condense on step edges. In the high-temperature γ phase of Fe ($\approx 910-1390^\circ\text{C}$) the solubility of Cu amounts to a maximum value of 8 at.%.¹⁷ We cannot rule out, therefore, that some of the removed Cu atoms are incorporated in the Fe crystallites.

The electronic states of the thicker Fe films (e.g., for $\Theta=5$) are clearly different from those of bcc Fe films on W(110).¹⁸ In the latter work the AREDC's exhibited two structures below E_F , which in a spin-resolved analysis could be assigned to emission from the majority and the minority spin component of ferromagnetic bcc Fe. The presence of only one component in our AREDC's is an indication that the minority spin bands as probed with $h\nu=21.22$ eV are located above E_F . Here we assume that the thicker films have a ferromagnetic order as has been shown by Kümmerle and Gradmann² and later by Rau *et al.*⁴ Structural order at this coverage is visible in our AREDC's by the presence of a small dependency of the peak position on the polar angle of emission. We consider the AREDC's from Fe/Cu(111) for $\Theta=5$ to be characteristic for bulk fcc Fe(111). We did not find an indication for 2D behavior in the electronic states.

For the thinner films ($\Theta=1$) we did not find a definite maximum of emission distinctly below E_F or any fine-structure detail. Although the film is certainly composed of islands, their thickness will not yet be sufficient for development of the bulk electronic structure. We conclude, therefore, that the results are characteristic for a 2D thin film of fcc Fe with an average thickness of more than one ML (but not yet corresponding to bulk fcc Fe). In such a film the majority spin bands (in case of ferromagnetic order) may have shifted towards E_F or the minority spin bands downwards, which would qualitatively explain the observed shape of the AREDC's. In both cases the magnetic properties should be different as compared to $\Theta=5$. That modifications in the magnetic structure of γ -Fe(111) films with the thickness are possible has been shown by Rau *et al.*, who found short-range ferromagnetic order up to $\Theta=2$ and long-range ferromagnetic order for thicker films.⁴

V. CONCLUSION

Out STM measurements have established the 3D nature of the growth of Fe films on Cu(111) up to a coverage of 4 ML for deposition at RT up to 300°C. A preferential condensation of the Fe islands at step edges on the

upper terrace is observed. Coalescence of the 3D Fe islands has not yet been reached for the maximum coverage ($\Theta=4$) used in the STM experiments. Regular islands with the threefold symmetry of the substrate are particularly found for deposition on a substrate, which is heated to 150 and 300°C. Symmetry of the islands and their orientation on the substrate can only be explained by the growth of the deposit in form of fcc Fe(111) layers. For small coverages an Fe-induced formation of holes in the Cu substrate and of 2D Cu islands in the vicinity of step edges is observed. The general growth mode as seen by STM is confirmed by the ARUPS results. We conclude that the AREDC's from a 1-ML and a 5-ML Fe deposit are representative for a 2D fcc Fe(111) film and bulk fcc Fe(111), respectively. We observe distinct differences in the AREDC's from both films, which indicate a downward shift of electronic states with increasing film thickness.

ACKNOWLEDGMENTS

This work has been supported by the Deutsche Forschungsgemeinschaft through Forschergruppe "Modelkat" and SFB 166.

¹C. Kittel, *Introduction to Solid State Physics*, 5th ed. (Wiley, New York, 1976).

²W. Kümmerle and U. Gradmann, *Phys. Status Solidi A* **45**, 171 (1978).

³R. Halbauer and U. Gonser, *J. Magn. Magn. Mater.* **35**, 55 (1983).

⁴C. Rau, C. Schneider, G. Xing, and K. Jamison, *Phys. Rev. Lett.* **57**, 3221 (1986).

⁵U. Gradmann and P. Tillmanns, *Phys. Status Solidi A* **44**, 539 (1977).

⁶Y. Darici, J. Marcano, H. Min, and P. A. Montano, *Surf. Sci.* **195**, 566 (1988).

⁷D. Tian, F. Jona, and P. M. Marcus, *Phys. Rev. B* **45**, 11216 (1992).

⁸P. Heimann and H. Neddermeyer, *Phys. Rev. B* **18**, 3537 (1978).

⁹The STM results on Fe/Cu(111) are briefly described by A. Brodde and H. Neddermeyer, *Ultramicroscopy* **42-44**, 556 (1992). We note, however, that a wrong step height for bcc Fe(110) has been used in the latter report. Actually, the step

heights on bcc Fe(110) and fcc Fe(111) are both close to 2 Å, which means that the step height cannot be used to distinguish between a bcc Fe(110) and a fcc Fe(111) layer.

¹⁰Th. Berghaus, A. Brodde, H. Neddermeyer, and St. Tosch, *Surf. Sci.* **184**, 273 (1987).

¹¹P. Heimann, J. Hermanson, H. Miosga, and H. Neddermeyer, *Phys. Rev. B* **20**, 3059 (1979).

¹²A. Brodde, G. Wilhelmi, D. Badt, H. Wengelnic, and H. Neddermeyer, *J. Vac. Sci. Technol. B* **9**, 920 (1991).

¹³Th. Michely, K. H. Besocke, and G. Comsa, *Surf. Sci.* **230**, L135 (1990).

¹⁴A. Brodde and H. Neddermeyer, *Surf. Sci.* (to be published).

¹⁵P. Heimann, H. Neddermeyer, and H. F. Roloff, *J. Phys. C* **10**, L17 (1977).

¹⁶P. Heimann, J. Hermanson, H. Miosga, and H. Neddermeyer, *Surf. Sci.* **85**, 263 (1979).

¹⁷W. B. Pearson, *Lattice Spacing and Structures of Metals and Alloys* (Pergamon, Oxford, 1958).

¹⁸R. Kurzawa, K.-P. Kämper, W. Schmitt, and G. Güntherodt, *Solid State Commun.* **60**, 777 (1986).

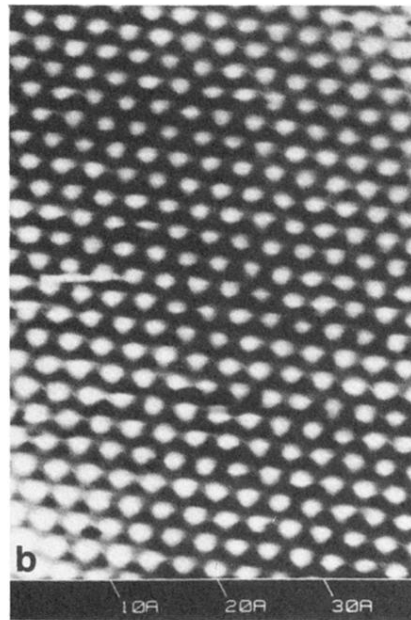
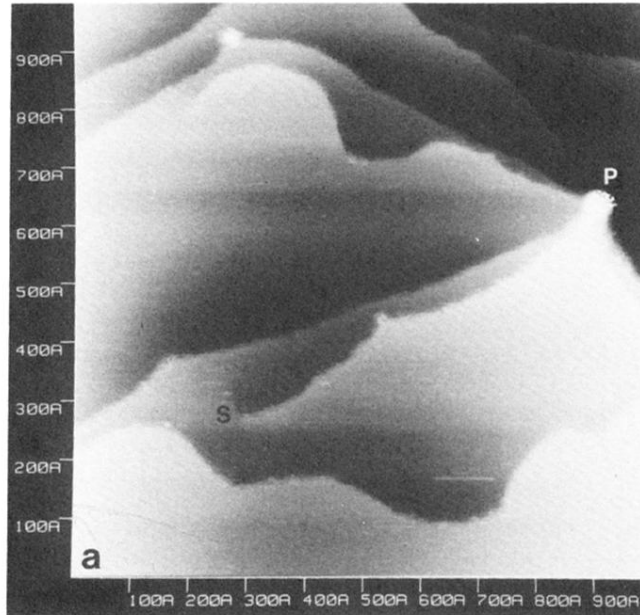


FIG. 1. CCT from clean Cu(111) acquired with $U = -0.1$ V and $I = 0.5$ nA (a) and $U = -1.25$ V and $I = 0.5$ nA (b).

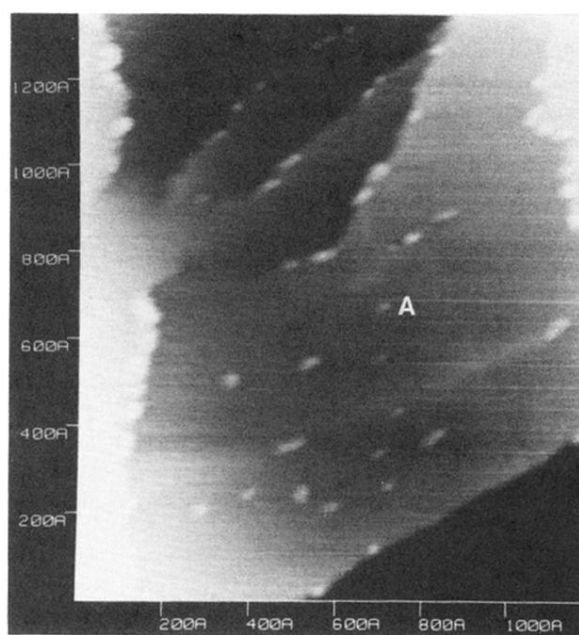


FIG. 2. CCT from 0.03-ML Fe on Cu(111) deposited at RT acquired with $U = -0.05$ V and $I = 0.5$ nA.

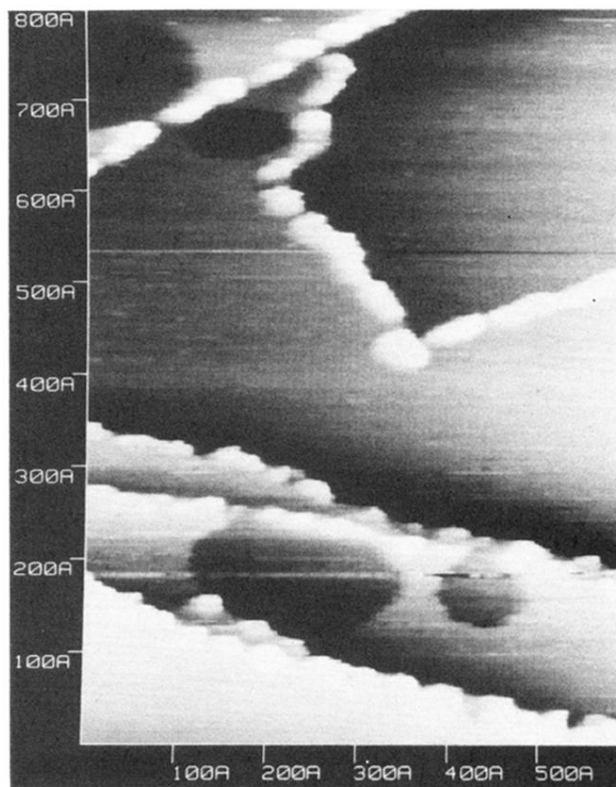


FIG. 3. CCT from 0.05-ML Fe on Cu(111) deposited at RT acquired with $U=0.05$ V and $I=0.5$ nA.

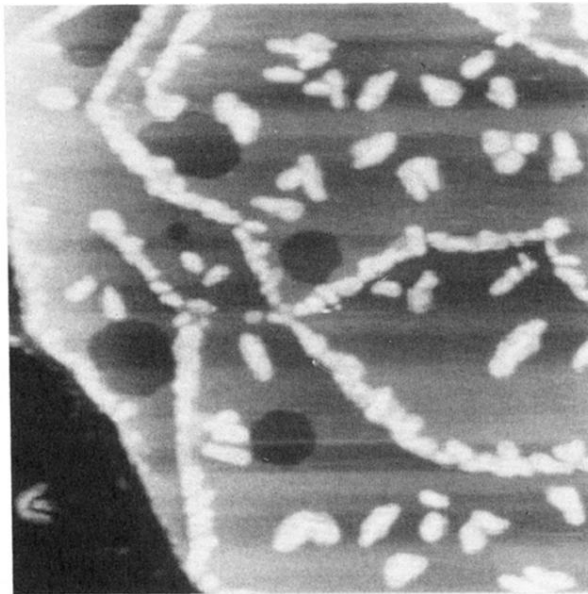


FIG. 4. CCT from 0.5-ML Fe on Cu(111) deposited at RT acquired with $U=0.05$ V and $I=0.5$ nA. The surface area is $2000 \times 2000 \text{ \AA}^2$.

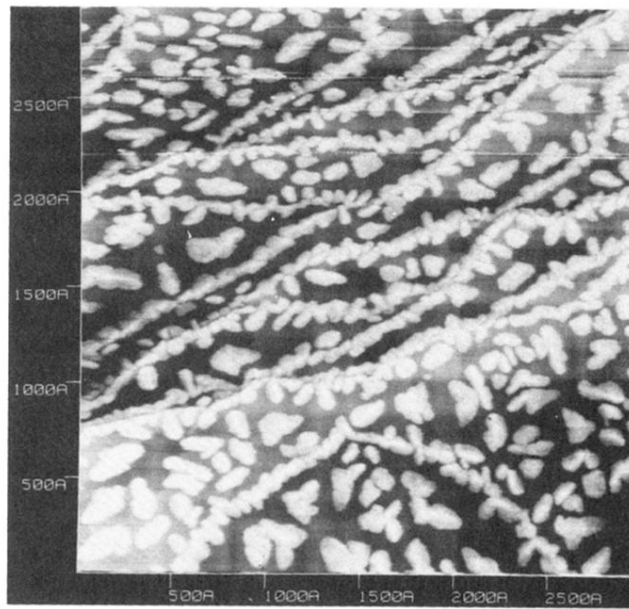


FIG. 5. CCT from 2-ML Fe on Cu(111) deposited at RT acquired with $U = 0.05$ V and $I = 0.5$ nA.

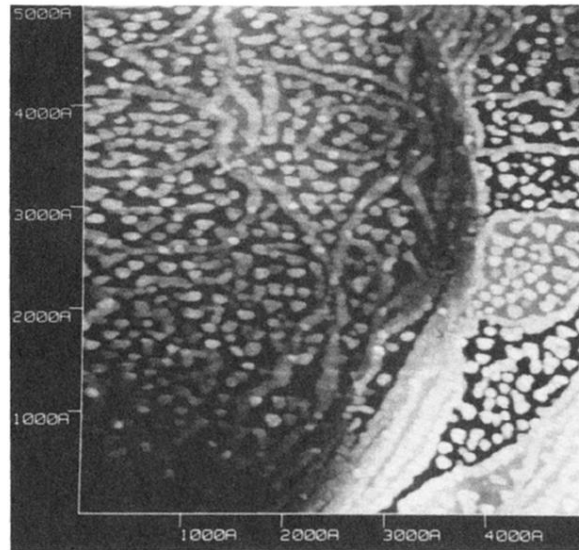


FIG. 6. CCT from 4-ML Fe on Cu(111) deposited at 300°C acquired with $U = -0.1$ V and $I = 0.5$ nA.

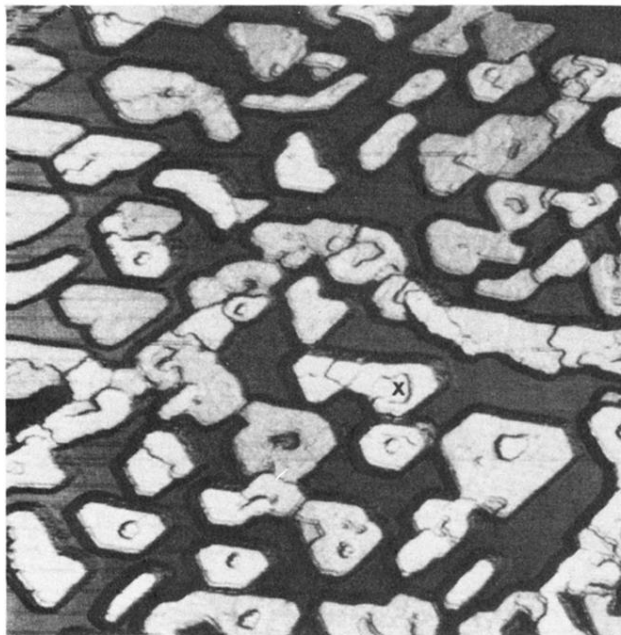


FIG. 7. CCT from 3-ML Fe on Cu(111) deposited at 150°C acquired with $U = -0.05$ V and $I = 0.5$ nA. The surface area is $1500 \times 1500 \text{ \AA}^2$. The uncovered Cu(111) substrate is represented in the intermediate gray tone level.

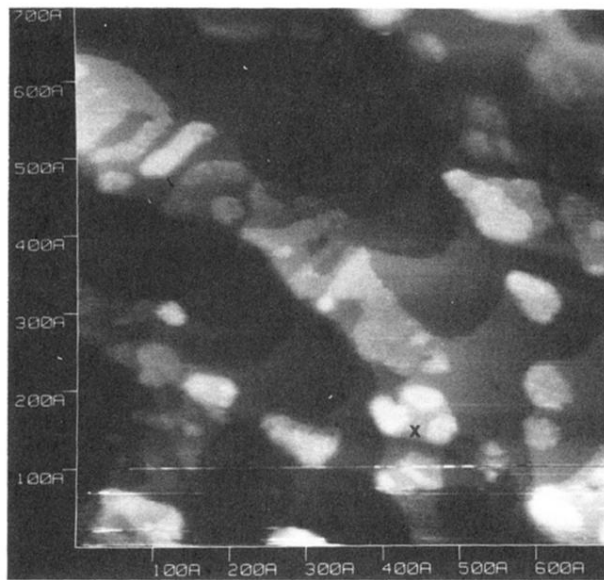


FIG. 8. CCT from ≈ 1 -ML Fe (the local coverage is smaller, in our opinion) on Cu(111) deposited at 150°C acquired with $U = -0.05$ V and $I = 50$ nA.